Journal of Al-Azhar University Engineering Sector

Vol.15, No. 55, April, 2020, 546-559

ENHANCEMENT OF HIGH-VOLTAGE RIDE-THROUGH OF A GRID-CONNECTED SWITCHED RELUCTANCE GENERATOR (SRG) WIND TURBINE USING A DYNAMIC VOLTAGE RESTORER BASED ON FUZZY LOGIC CONTROLLER

M. Bahy*[1], M. A. Morsy Shanab[1], Adel S. Nada[2] and S. H. Elbanna[2]
[1]Electrical Power and Machines Dep, The Higher Institute of Engineering at El-Shorouk City, Cairo, Egypt.
[2]Electrical Engineering Dep, Faculty of Engineering, AL-Azhar University, Cairo, Egypt.
*Correspondence Author: Email: eng.mohamedbahy@gmail.com

ABSTRACT
This paper proposes a Fuzzy Logic Controller (FLC) of Dynamic Voltage Restorer (DVR) to enhance the capability of High voltage Ride-Through (HVRT) for a wind turbine based on a Switched Reluctance Generator (SRG). Voltage Swell on the grid side may cause the wind turbine to be disconnected from the grid. Two FLCs are used to regulate the IGBT pulses of the voltage source inverter (VSI) driving DVR by adjusting the D-Q axes voltage signals. To validate the effectiveness of the DVR based FLC, three test scenarios are investigated includes (balanced swell, unbalanced swell, and total harmonics distortion).The enhancement of the system performance is achieved through improving the voltage, the current as well as the power waveforms for the wind turbine and fulfill the grid codes without disconnecting the turbine from the grid. The proposed system is modeled using MATLAB/Simulink.

KEYWORDS: Switched Reluctance Generator (SRG), Dynamic Voltage Restorer (DVR), High Voltage Ride-Through (HVRT), Fuzzy Logic Control (FLC).

تعزيز ركوب الجهد العالي لتوربينات الرياح المتصلة بالشبكة من خلال مولد المعاوقة ذات الفصل والتوصيل باستخدام المرمم الديناميكي للجهد المبني بوحدة التحكم المنطقي المبهم

محمد بهي*[١] و محمد احمد مرسي شنب[١]وعادل سعد ندا[٢] و سيد حسني البنا[٢]
[١]قسم الهندسة والآلات الكهربية ، المعهد العالي للهندسة بمدينة الشروق، القاهرة، مصر
[١]قسم الهندسة الكهربية، كلية الهندسة، جامعة لأزهر، القاهرة، مصر
*البريد الاليكتروني للباحث الرئيسي: Email: eng.mohamedbahy@gmail.com

الملخص
يقدم هذا البحث وحدة تحكم منطقي مبهم لمرمم الجهد الديناميكي لتعزيز قدرة ركوب الجهد العالي لتوربينات الرياح على أساس مولد المعاوقة ذو الفصل والتوصيل. قد يؤدي تضخم الجهد على جانب الشبكة إلى فصل توربينات الرياح عن الشبكة. يتم استخدام اثنين من وحدات التحكم المنطقي المبهمة لتنظيم نبضات لعاكس مصدر الجهد الذي يقود مرمم الجهد الديناميكي عن طريق ضبط إشارات الجهد. للتحقق من فعالية مرمم الجهد الديناميكي المستندة إلى التحكم المنطقي المبهم ، يتم فحص ثلاثة سيناريوهات اختبار (تضخم الجهد المتوازن ، تضخم الجهد غير المتوازن ، وتشويه التوافقيات الكلي. يتم تحسين أداء النظام من

خلال تحسين أشكال موجات الجهد و التيار وكذلك القدرة لتوربينات الرياح والوفاء برموزالشبكة دون فصل التوربينات عنها. تم تصميم النظام المقترح باستخدام متلاب سيمولينك.

الكلمات المفتاحية: مولد المعاوقة ذو الفصل والتوصيل ، مرمم الجهد الديناميكي ، ركوب الجهد العالي، التحكم المنطقي المبهم.

1. INTRODUCTION

Wind energy generation has been noted as the most rapidly growing renewable energy technology. The rapid deployment of wind power plants (WPPs) has made grid integration and operational issues focal points in industry discussions and research [1]. The Switched Reluctance Generator (SRG) is a good alternative for wind generation applications because of its operating characteristics, which allow it to function in a wide range of speed at high-performance levels [2]. Besides, the SRG has attractive features, such as mechanical robustness, high performance, low fabrication cost, and the absence of permanent magnetic elements [3], [4], [5]. The increasing penetration level of wind energy can have a significant impact on the grid, especially High Voltage Ride-Through (HVRT) conditions.

The impact of voltage dip on Wind Turbine (WT) and its Low Voltage Ride-Through (LVRT) technology are common studied currently [6]. However, the impact of grid voltage swell on WT and the corresponding HVRT have not been given sufficient attention. In actual WPPs, a voltage swelling is the brief increases in voltage over the time range from milliseconds to a few seconds. Among the grid disturbances, a voltage swell is a critical event that can be caused by abrupt switching off large loads or switching on capacitive load or damaged/loose neutral connection in the power system.

Currently, SRG is used mostly and its stator is connected to the grid through the converter [2]. Therefore, similar to the grid voltage dip, the transient process will also format current and voltage shocks to the stator of SRG when the grid voltage swell. To circumvent these problems and protect the converter, a wind turbine should automatically off-grid and then connect to the grid after the recovery of the grid, but this off-grid strategy does not satisfy the scale wind power in today's grid-connected standards and requirements.

Among the modern grid codes for wind energy grid integration, (LVRT) capability is considered under transient conditions and providing the grid by reactive currents as specified in the grid codes (e.g., of China GB/T 19963 [7], and of United States' Federal Energy Regulatory Commission (FERC) [7], [8]). During the HVRT, The time requirements in Figure 1 are displayed, if so the PCC voltage is below the HVRT line, the WTGs should be able to connect to the power grid. WTGs can be as well cut off from the power grid only if the PCC voltage exceeds the HVRT LINE [7].

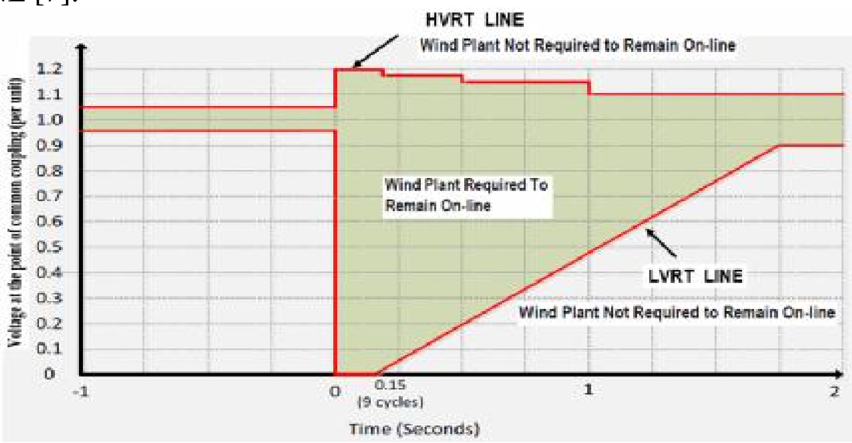

Fig. 1. Voltage requirements through LVRT and HVRT at PCC in ERCOT (ERCOT Nodal Operating Guides)

Many types of equipment are available to comply with the LVRT grid codes. Series Flexible AC Transmission Systems (FACTS) devices as for example dynamic voltage restorer (DVR), Thyristor-Controlled Voltage Regulator (TCVR) capable of injecting series voltage, super-conducting fault current limiters (SFCL) and Modulated Dynamic Braking Resistor Series (MSDBR) have desired performance to improve LVRT capability [9], [10]. Furthermore, increasing this capability with parallel equipment like Static Synchronous Compensator (STATCOM) is not cost-effective [11].

Figure 2(a) shows the proposed system in this paper. On the other hand, DVR used to mitigate the disturbance applied to the system as shown in Figure 2(b), DVR consists of energy storage, voltage source inverter, injection transformers, and L-C filters. The VSI will be controlled using two FL controllers. The DVR has the ability to attenuate voltage disturbances [12]. It is generally installed between the load and the source in the distribution system to provide rapid support of the voltage by injecting the required voltage in series with the mains voltage through an injection transformer [13]. A DVR is a good solution since no other protective circuit is needed in operation [14].

In [15], STATCOM connected to the PCC bus is applied to absorb reactive power from the grid to enhance the HVRT of the WTGS. Literature [16] proposes a control strategy for low voltage ride-through capability enhancement of a grid-connected switched reluctance wind generator. The adaptive PI controllers were successfully applied to control the power electronic circuits. The adaptation algorithm is based on the Widrow-Hoff delta rule. It is shown that the controller design significantly improves the wind turbine fault ride-through capability.

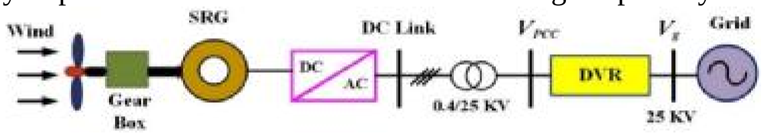

(a) Wind system with DVR.

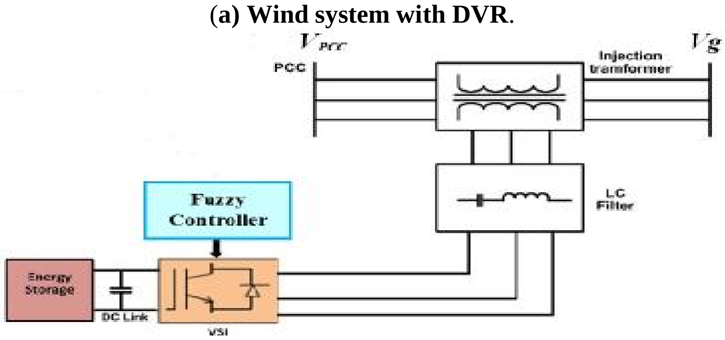

(b) DVR components.

Fig. 2. (a) Block diagram of Wind system with DVR and (b) DVR components.

Authors in [17] have used the DVR with combined Feed-Forward and Feed-Back (CFFFB) control using voltage control based on the proportional-integral (PI) controller. The output voltage measured of the DVR (or load voltage) is fed back to the voltage controller to produce of Voltage Source Inverter (VSI) switching pulses in the CFFB system. The PI control scheme displays simplicity and easy to implement. It is also not suitable for systems with changing parameters and operating conditions because of their fixed gains [18].According to the analysis of the above literature, a DVR based on FLC is employed in this paper to overcome the deficiencies of the PI controller under various fault conditions such as balanced voltage swell and unbalanced voltage swell. The results of the simulation show that DVR can enhance the SRG terminal voltage during HVRT on the grid by using MATLAB/SIMULINK software.

2. MATHEMATICAL MODEL OF THE SRG

An SRG is a machine that a doubly salient pole supplied by unipolar power converters [3]. The configuration of a 3-phase machine with 12 poles on the stator and 8 poles on the rotor is displayed in Figure 3(a). The asymmetric half-bridge (AHB) converter for a three-phase SRG is shown in Figure 3(b), when the switches are turned on, the phase is excited and energy is saved in the magnetic field. Turning off the switches leads to the transmission of the generated electric power to the grid through freewheeling diodes. For the determination of the dynamic characteristics of the SRG using MagNet Software, it is necessary to establish an appropriate coupling between the external electric circuit and the finite element model model.

The average electric power of SRG phases (*Pout*) is the summation of the output power of each phase in one electric cycle [19]

$$P_{out} = \frac{1}{T} \sum_{j=1}^{N_s} \int_0^T v_j \; i_j \; dt \qquad (1)$$

Where N_s, T , v_j , i_j are the number of motor phases, the conduction period of one phase, voltage and current of Phase *j*. It must be remembered that each phase of the SRG, ideally, can be considered as a de-coupled magnetic circuit, whose dynamics are given by its phase voltage differential equation.

$$v_j = R\, i_j + \frac{d\lambda_j}{dt} \qquad (2)$$

Where R is the winding resistance per phase, λ_j represents the flux linkage of Phase j due to the current i_j, and t is time. The phase flux linkage λ_j is given by

$$\lambda_j = L_j(i_j, \theta)\, i_j \qquad (3)$$

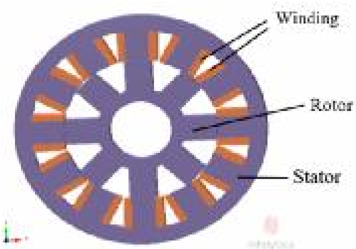

Fig. 3. (a) Machine structure

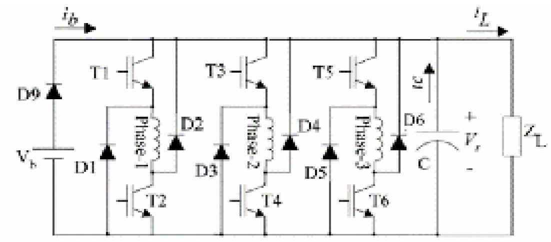

Fig. 3. (b) Asymmetric half bridge converter for a 3-ph SRG

Using MATLAB/SIMULINK software, the behavior of the SRG under normal operation of the system is shown in Figure 4. Figure 4(a) shows the output voltage generated by the WT-SRG, Fig. 4(b) shows the output current of SRG and Figure4(c) shows the active power generated by the WT-SRG.

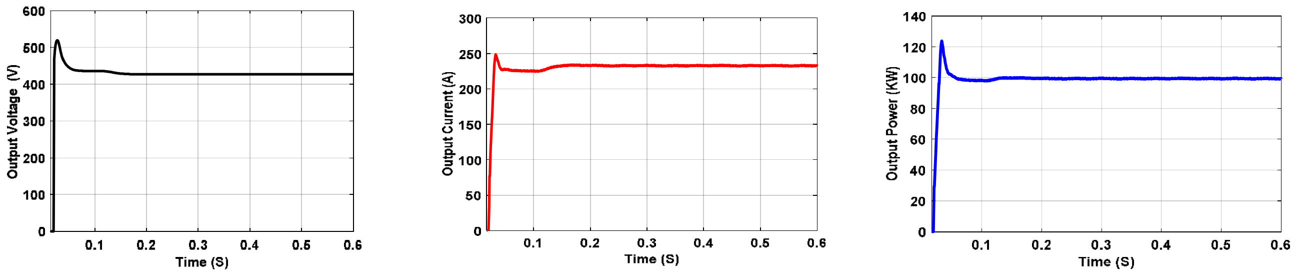

(a) (b) (c)

Fig. 4. ehavior of the SRG under normal operation of the system. (a) Output voltage of SRG in V. (b) Output current of SRG in A. (c) Active power of SRG in Kw

3. DYNAMIC VOLTAGE RESTORER (DVR)

The proposed DVR consists of energy storage, voltage source inverter, LC filter, injection transformer as shown in Figure 2(b). The energy storage feed voltage source inverter which injects a suitable voltage to restore the load voltage by using an injected transformer. Controllable AC supply is obtained from VSI, due to IGBT, the output includes some harmonics so that the LC filter is used to mitigate this problem [20], [21]. When any disturbance is applied V_g, the DVR will inject an appropriate voltage through an injection transformer to mitigate this disturbance. The DVR will treat with these disturbances and inject an appropriate voltage to mitigate the problem and released a cleared sinusoidal and balanced wave from distortions and effects of disturbance that emerged in the system.

3.1 Control Techniques of DVR

The important and essential part of the DVR system is the controller. To control the DVR system, a closed-loop control in a rotating DQ reference frame is introduced in [22],[14], when disturbances occur, the DVR controller injects a suitable pulse for IGBT of VSI. Figure 5 illustrates the control Scheme of DVR. The ABC three-phase coordinate system is converted into the dq0 coordinate system by the following equations [21]:

$$V_d = \frac{2}{3}\left[V_a \sin\omega t + V_b \sin\left(\omega t - \frac{2\pi}{3}\right) + V_c \sin\left(\omega t + \frac{2\pi}{3}\right)\right] \quad (4)$$

$$V_q = \frac{2}{3}\left[V_a \cos\omega t + V_b \cos\left(\omega t - \frac{2\pi}{3}\right) + V_c \cos\left(\omega t + \frac{2\pi}{3}\right)\right]$$

(5)

$$V_o = \frac{1}{3}[V_a + V_b + V_c] \quad (6)$$

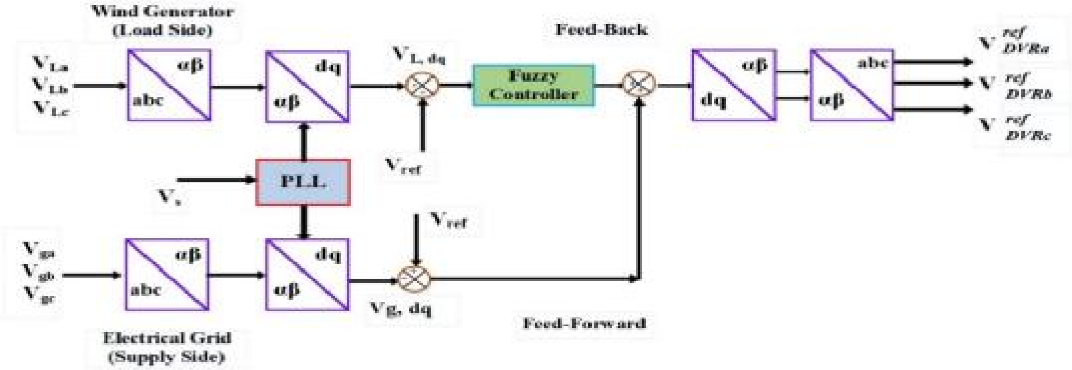

Fig. 5. The control scheme of DVR with FLC

The disturbance that occurred in the DQ coordinate will be calculated by comparing the DQ with a reference value, then it's converted to ABC again. On the other hand, the phase-locked loop (PLL) is used to measure the system frequency. The error between the actual values and reference values of DQ voltage is used as input to the FLC of DVR as shown in the following equations:

$$error_d(t) = [V_{dref} - V_d] \quad (7)$$

$$error_q(t) = [V_{qref} - V_q] \quad (8)$$

The $error_d$ signal is used as an input to the D-axis FLC and $error_q$ is used as an input to the Q-axis FLC. The output is converted to ABC coordinates, then it is directed to the PWM to give appropriate pulses for the IGBT of VSI. The load voltage (V Load) is measured, then transformed to dq0 coordinates, the error between the dq voltages and a reference voltage of DQ coordinates represents the input of FLC, the d reference is 1 p.u. (rated voltage) and q reference is 0. Two FLCs are used for d and q error signals FLC_d, FLC_q respectively. The output of the FLC is transformed to ABC then forwarded to PWM for triggering IGBT of VSI.

3.1.1 Fuzzy Control Strategy

Nonlinear controllers such as FLC are more suitable to control applications of power systems [23]. They are designed and implemented easily and can adjust to a greater variety of operating conditions. Self-organized fuzzy controllers can refine the membership functions automatically [12]. Conventional process-based control techniques involve a linear model of the system and cannot guarantee good performance across a wide range of operations.
The Fuzzy process operates through two stages: Fuzzificaton and Defuzzification. Fuzzification is the process of transforming the crisp input to a fuzzy value. The fuzzy output is developed using the rules. FLC is structured on fuzzy control rules which use the value of fuzzy sets generally for error and change of error and control action. Defuzzification is the process of combining the results to provide a crisp output controlling the output variable [24]. Table 2 displays the error signal sign and the linguistic code output. Error and derivative of error are exits in FLC with seven linguistic variables. Which is; Positive-Big (PB), Positive-Medium (PM), Positive-Small (PS), Zero (ZE), Negative-Small (NS), Negative-Medium (NM), and Negative-Big (NB).

Table. 1 Rules for Fuzzy Controllers

Ce \ e	**NB**	**NM**	**NS**	**ZE**	**PS**	**PM**	**PB**
NB	NB	NB	NB	NB	NM	NS	ZE
NM	NB	NB	NB	NM	NS	ZE	PS
NS	NB	NB	NM	NS	ZE	PS	PM
ZE	NB	NM	NS	ZE	PS	PM	PB
PS	NM	NS	ZE	PS	PM	PB	PB
PM	NS	ZE	PS	PM	PB	PB	PB
PB	ZE	PS	PM	PB	PB	PB	PB

Figure 6 shows the partition of Fuzzy subsets and the form of the membership functions. The triangular shape of this arrangement's membership functions presumes that there is only one dominant fuzzy subset for any particular input.

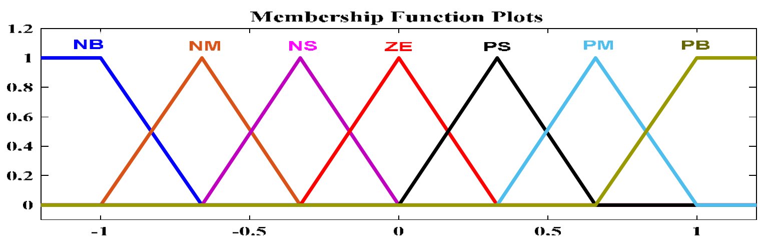

Fig. 6. The membership functions for input signals e, c_e and output u

4. SIMULATION RESULTS AND DISCUSSION

The results of the simulation under HVRT with DVR are discussed. The presented DVR is investigated in the MATLAB/Simulink platform in terms of enhancing balanced and unbalanced voltages swell, for the power system shown in Figure 7, the designed DVR has the power of 1 MVA to regulate the voltage of a 100 Kw SRG based on WT connected to the 25 kv distribution network. The DVR adjusts the voltage at buses B-Grid and B-PCC by injecting an appropriate voltage. The leakage reactor of the coupling transformer produces this voltage-transfer by producing a secondary voltage in phase with the primary voltage (gate side).

The DVR during normal operation is in standby mode. If the fault occurs, the control system detects the voltage disturbance in supply and then, as will be explained in all cases, the required voltage is injected by the DVR. During various fault conditions, the effects of transient active power, transient voltage, transient current, DC output voltage of SRG and harmonics performance in terms of % THD are discussed in detail. The SRG and DVR simulation parameters are given in Table 2. The results for the PCC are given where the simulations are provided with the proposed DVR based on FLC and DVR based on the PI controller.

For the following cases, the WT HVRT performance will be assessed and analyzed:

Case 1: Balanced voltage swell of 1.5 p.u.

Case 2: Unbalanced voltage swell of 1.5 p.u.

Case 3: Harmonics spectrum analysis.

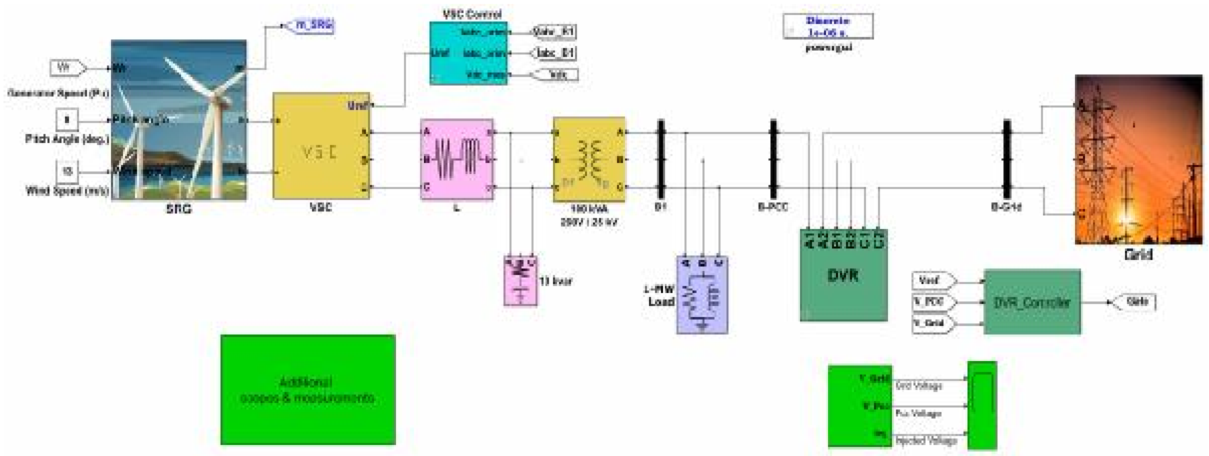

Fig. 7. MATLAB simulation model of the system under study.

Table 2. Simulation parameters for SRG and DVR.

DVR parameters	Value	SRG parameters	Value
V_{DC}	3000 V	Rated voltage	600 V
R	0.1 Ω	Torque	650 N.m
Voltage source inverter	3 arms, 6 pulses	Output power	100 kW
Carrier frequency	5000 Hz	Stator poles	12
Filter shunt resistance	60 Ω	Rotor poles	8
Filter shunt capacitance	6 µF	Base speed	1200 r.min^{-1}
Filter series inductance	80 mH	Resistance per phase	0.03109 Ω
Filter series resistance	0.1 Ω	Moment of inertia	0.05 kg.m^2
Boosting transformer ratio	1:1	Friction coefficient	0.02 N.m.s

4.1 Case 1: Three-Phase Balanced Voltage Swell

Swelling occurs because the heavy loads in three phases are switched off. Therefore, for this test, the symmetrical voltage swelling of 150 % with respect to V_{ref} is created in the grid side at t = 0.2 s. for 0.2 s duration (10 cycles at 50HZ). When connecting the DVR to the PCC and the same voltage swelling is created; in that case, DVR injects the required voltage on the three phases and then enhances the system's PCC voltage profile. Figure 8(a) shows the grid side balanced swell voltage in volts. The PCC voltage in Volts is shown in Figure 8(b) after compensation and Figure 8 (c) shows DVR injection voltage in Volts.

The transient behaviors of the studied SRG wind turbine are simulated and compared, respectively during a swell mode with DVR-based series compensation using both control schemes with FLC and PI controller. The dynamic responses of the system studied are shown in Figure 9 during this swell mode. The results of the simulation in Figure 9 (a) shows that voltage magnitude in p.u. at PCC during the swell mode, As a result, the voltage is closely regulated to 1 p.u. with small overshoot below the safety limits for both control schemes. It is also observed that overshooting and oscillation can be minimized more effectively with the FLC scheme compared to the PI controller scheme. The output voltage of SRG in Volts is shown in Figure 9(b). After 1 cycle of oscillations, which corresponds to approximately 0.02 s, the voltage reaches the steady-state with a small overshoot.

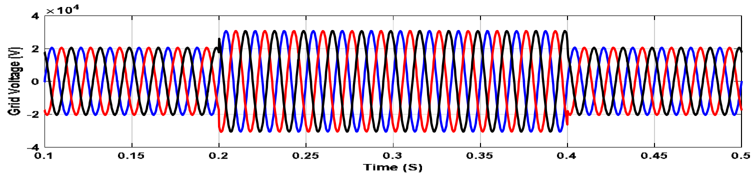

(a)

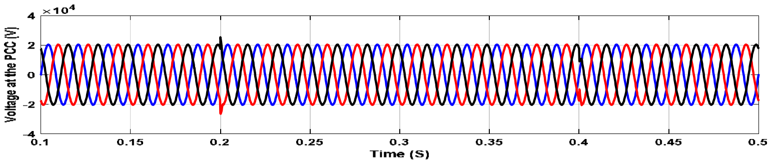

(b)

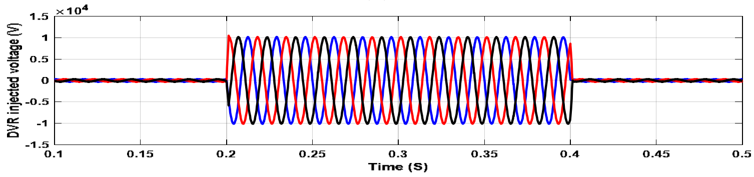

(c)

Fig. 8. Simulated results for case 1: Balanced swell mode by using DVR based on FLC (a) Grid voltage in volts, (b) compensated PCC voltage in volts, and (c) DVR injected voltage in volts

Figure 9(c) indicates the current injected into the grid at PCC from the SRG wind turbine. If the DVR is absent, the current dropped from 230 A to 125 A until the end of a swell disturbance where large oscillations appeared. The current decrease from 230 A to 225 A can also be seen. With small overshoots and oscillations for 0.04 s and is then completely damped using DVR based on FLC. The active power produced by the WT based on SRG at the PCC is shown in Figure 9 (d). During the swell disturbance, if the DVR is absent, the active power dropped from 100 Kw to 60 kw with large oscillations until the swelling period ended. DVR based on FLC reduces overhead and oscillating active power and is fully damped after 0.04 s.

These standards have been agreed on for the results of a simulation. The time of recovering of these values is well within the recovery limits as displayed in the grid code curves of Figure 1. The simulation results show that the DVR based series compensation using FLC works effectively to prevent the SRG wind turbine from transient voltages and currents.

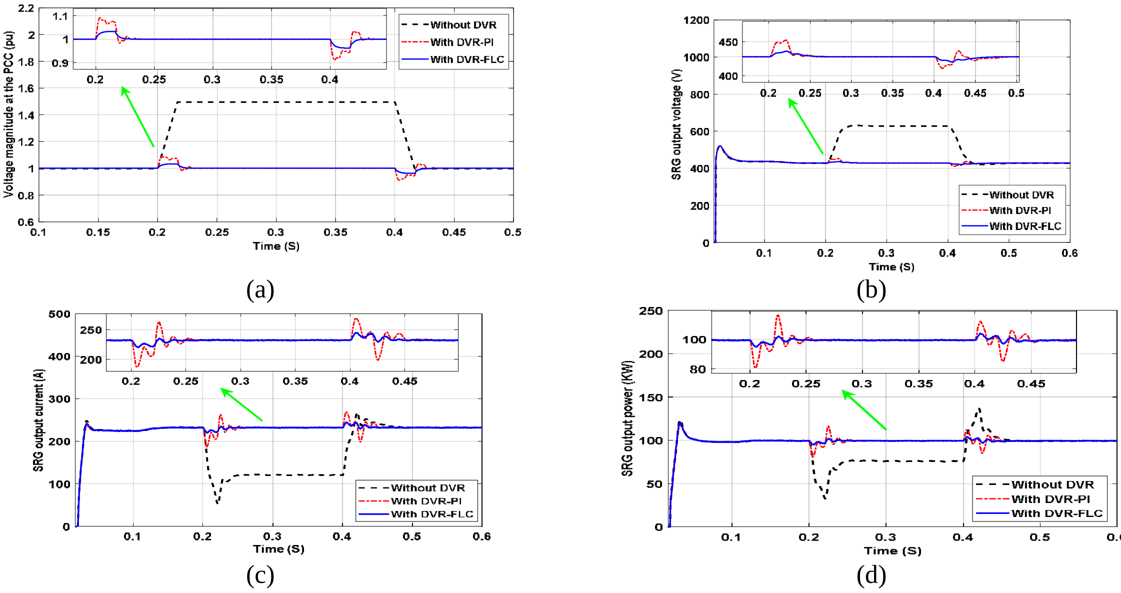

Fig. 9. (a) Voltage magnitude at PCC with 150 % balanced swell using DVR based on FLC, with PI and without DVR in p.u. (b) The output voltage of SRG with 150 % balanced swell using DVR based on FLC, with PI and without DVR in Volts. (c) The output current of SRG with 150 % balanced swell using DVR based on FLC, with PI and without DVR in A. (d) Active power of SRG with 150 % balanced swell using DVR based on FLC, with PI and without DVR in Kw.

4.2 case 2: Three-Phase Unbalanced Voltage Swell

In this case, an unbalanced voltage swell of 150% with respect to the reference voltage occurs from 0.2 s to 0.4 s (10 cycles at 50HZ) in the system in phase A. It can be observed that the DVR rapidly detects this case in phase A and injects the necessary magnitude and phase angle of voltage to keep PCC in balance. Figure. 10 depicts the load voltage profile before and after compensation as well as the necessary injected voltage. Figure 10(a) shows the grid side unbalanced swell voltage in volts.

The PCC voltage in Volts is shown in Figure 10(b) after compensation and Figure 10(c) shows DVR injection voltage in Volts. The transient behaviors of the SRG wind turbine with DVR-based series compensation using both control schemes with FLC and PI controller are simulated and compared during the unbalanced swell mode.

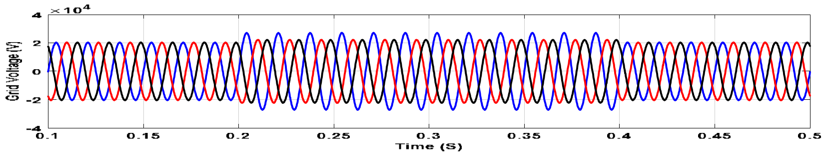

(a)

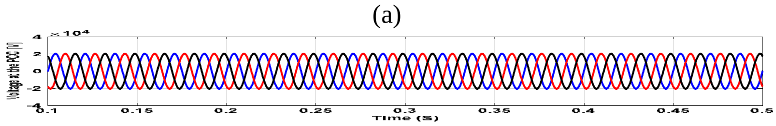

(b)

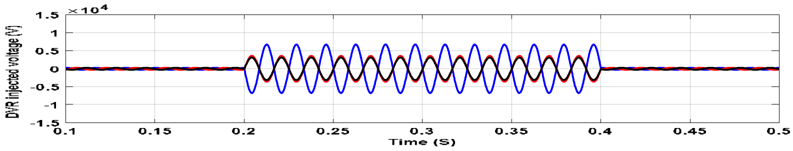

(c)

Fig. 10. Simulated results for case 2: Unbalanced swell mode by using DVR based on FLC (a) Grid voltage in volts, (b) compensated PCC voltage in volts, and (c) DVR injected voltage in volts

The dynamic responses of the system studied are shown in Figure 11 during the unbalanced swell mode. The voltage magnitude at the PCC is controlled to 1 p.u. without overshoot for the FLC scheme compared to the PI controller as illustrated in Figure 11 (a). The output voltage of SRG in Volts is illustrated in Figure 11 (b). The voltage reaches the steady-state without overshoot for the FLC scheme compared to the PI controller.

Figure 11(c) and Figure 11(d) shows the current and the power injected from the SRG wind turbine into the grid at PCC. Without the DVR, these figures show the large oscillations during the unbalanced swell disturbance period. It can also be seen that the current or power has not overshoots and oscillations for DVR based on FLC.

The results of simulation show that the DVR based series compensation using FLC works effectively to prevent the SRG wind turbine from transient voltages and currents. The time of recovering is well within the recovery limits as illustrated in the grid code curves of Figure 1.

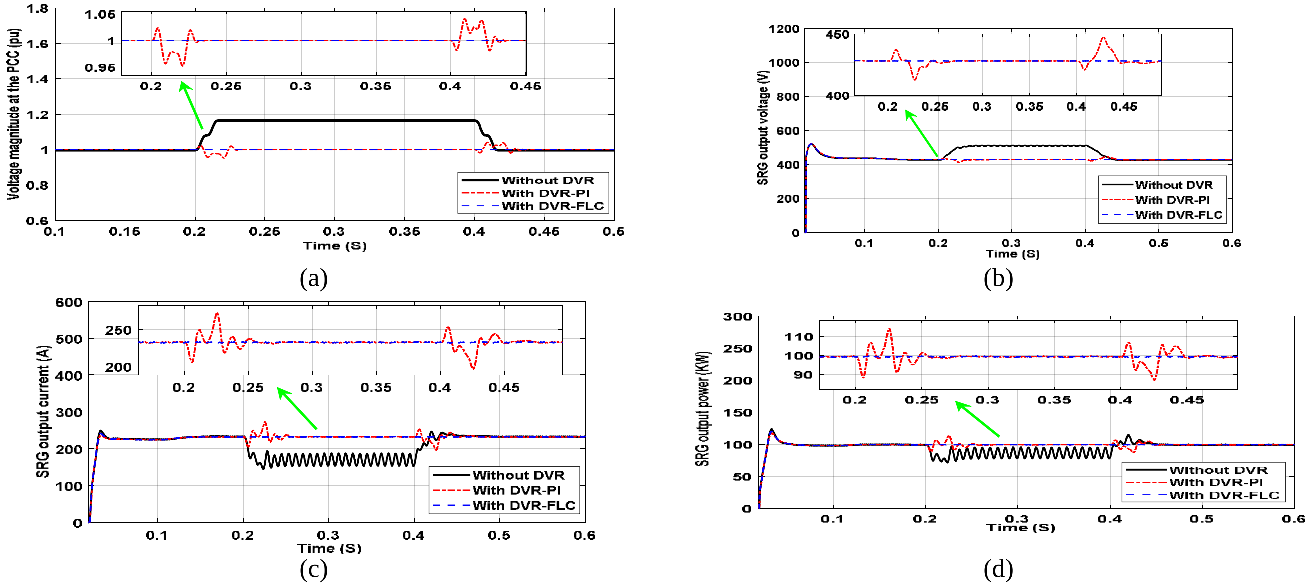

Fig. 11. (a) Voltage magnitude at PCC with 150 % unbalanced swell using DVR based on FLC, with PI and without DVR in p.u. (b) The output voltage of SRG with 150 % unbalanced swell using DVR based on FLC, with PI and without DVR in Volts. (c) An output current of SRG with 150 % unbalanced swell using DVR based on FLC, with PI and without DVR in A. (d) Active power of SRG with 150 % unbalanced swell using DVR based on FLC, with PI and without DVR in KW.

4.3 Case 3: Analysis of Harmonic Distortion

Total harmonics distortion (THD) has major negative implications for the system and most grid disturbances are followed by harmonics, Therefore it is important to measure the voltage or current waveforms level of harmonic distortion [25]. The THD values of the voltage and current at the source and load busses with the proposed DVR are therefore investigated.

Figure 12 depicts the measured THD of voltages and currents at the PCC during swell mode to verify the effectiveness of the proposed DVR schemes. It is clearly seen that the THD of the voltage and current values using DVR based on FLC are significantly reduced to be within the allowable limits stated in IEEE 519 [26]. The comparison shows a significant improvement in the performance of DVR using DVR based on FLC. DVR complies to operate within the acceptable limits of THD%.

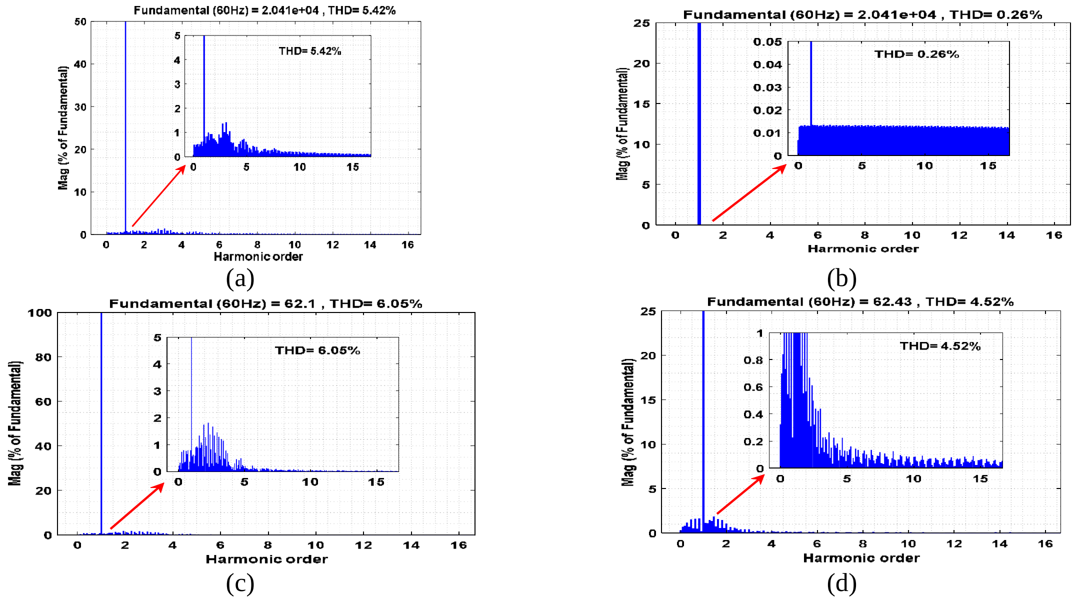

Fig. 12. FFT analysis of the voltages and currents at PCC bus: (a) THD_v at V_{PCC} with PI DVR during the swell mode, (b) THD_v at V_{PCC} with FLC DVR during the swell mode, (c) THD_i with PI DVR during the swell mode, (d) THD_i with FLC DVR during swell mode

5. CONCLUSION

This paper presented two FL controllers of DVR to improve the performance of SRG-based wind turbines to achieve HVRT. The DVR is connected between the PCC and the grid. The main idea behind the proposed controller is to regulate the injected DVR voltage to improve the voltage profile at the PCC at abnormal operating conditions. Results show that, at faulty conditions, DVR based FLC has the ability to mitigate the distortions in currents, voltages and power waveforms. In the three test cases introduced (balanced voltage swell, unbalanced voltage swell, and THD), by using DVR based FLC, there is a noticeable improvement in the waveforms and performance of the system. Moreover, an improvement in the wind turbine generator speed performance. In addition, the integration of controlled DVR proposed into SRG-based wind turbines also keeps the continuous operation of the WT at faulty conditions without the need for additional protection methods and meet any requirements for a grid code.

REFERENCES

1. Z. Wu, C. Zhu, M. Hu. (2013). “Improved control strategy for DFIG wind turbines for low voltage ride through”. Energies, vol. 6, no. 3, pp. 1181–1197.
2. T. A. S. Barros, P. J. S. Neto, P. S. N. Filho, A. B. Moreira, and E. Ruppert. (2016) “Approach for performance optimization of switched reluctance generator in variable-speed wind generation system”. Renew. Energy, vol. 97, pp. 114–128.
3. M. Bahy, A. S. Nada, S. H. Elbanna, M. A. M. Shanab. (2020). “Voltage control of switched reluctance generator using grasshopper optimization algorithm”. Int. J. Power Electron. Drive Syst, vol. 11, no. 1, pp. 75–85.
4. E. Rahmanian, H. Akbari, and G. H. Sheisi. (2017). “Maximum Power Point Tracking in Grid Connected Wind Plant by Using Intelligent Controller and Switched Reluctance Generator”. IEEE Trans. Sustain. Energy, vol. 8, no. 3, pp. 1313–1320.

5. T. Andre Santos Barros and E. Ruppert Filho.(2015). “Direct power control for switched reluctance. Generator in wind energy”. IEEE Lat. Am. Trans., vol. 13, no. 1, pp. 123–128.
6. Z. Xie, X. Zhang, S. Yang, H. Song, and T. Qu. (2012). “High voltage ride-through control strategy of doubly fed induction wind generators based on virtual impedance”. Zhongguo Dianji Gongcheng Xuebao/Proceedings Chinese Soc. Electr. Eng., vol. 32, no. 27, pp. 16–22.
7. D. Wenzhong Gao, E. Muljadi, T. Tian, and M. Miller. (2016). “Comparison of Standards and Technical Requirements of Grid- Connected Wind Power Plants in China and the United States”. no. September, p. 50.
8. “UNITED STATES OF AMERICA JOINT REPORT OF THE NORTH AMERICAN ELECTRIC RELIABILITY”. (2005). vol. 34993, no. 661.
9. [X. Chen, L. Yan, X. Zhou, and H. Sun. (2018). “A Novel DVR-ESS-Embedded Wind-Energy Conversion System”. IEEE Trans. Sustain. Energy, vol. 9, no. 3, pp. 1265–1274.
10. S. G. Liasi, Z. Afshar, M. J. Harandi, and S. S. Kojori. (2018). “An Improved Control Strategy for DVR in order to Achieve both LVRT and HVRT in DFIG Wind Turbine”. EPE 2018 - Proc. 2018 10th Int. Conf. Expo. Electr. Power Eng., pp. 724–730.
11. M. J. Ghorbanian, F. Goodarzvand, A. Pourdaryaei, and W. N. L. Mahadi. (2015). “Mitigating voltage sag by implementing STATCOM on DFIG-based wind farms connected to a power system”. 2014 4th Int. Conf. Eng. Technol. Technopreneuship, vol, pp. 131–136.
12. A. Benali, M. Khiat, T. Allaoui, and M. Denaï. (2018). “Power Quality Improvement and Low Voltage Ride Through Capability in Hybrid Wind-PV Farms Grid-Connected Using Dynamic Voltage Restorer”. IEEE Access, vol. 6, pp. 68634–68648.
13. D. D. Lu. "AN UPDATE ON POWER QUALITY Edited by Dylan Dah-Chuan Lu".
14. C. Wessels, F. Gebhardt, and F. W. Fuchs. (2011). “Fault ride-through of a DFIG wind turbine using a dynamic voltage restorer during symmetrical and asymmetrical grid faults”. IEEE Trans. Power Electron., vol. 26, no. 3, pp. 807–815.
15. Y. M. Alharbi, A. M. Shiddiq Yunus, and A. Abu-Siada. (2011). “Application of STATCOM to improve the high-voltage-ride-through capability of wind turbine generator”. 2011 IEEE PES Innov. Smart Grid Technol. ISGT Asia 2011 Conf. Smarter Grid Sustain. Afford. Energy Futur., pp. 5–9.
16. H. M. Hasanien, S. M. Muyeen, and A. Al-Durra. (2016). “Adaptive control strategy for low voltage ride through capability enhancement of a grid-connected switched reluctance wind generator”. IET Conf. Publ., vol. 2016, no. CP694, pp. 1–6.
17. A. Rini Ann Jerin, N. Prabaharan, K. Palanisamy, and S. Umashankar. (2017). “FRT Capability in DFIG based Wind Turbines using DVR with Combined Feed-Forward and Feed-Back Control”. Energy Procedia, vol. 138, pp. 1184–1189.
18. E. El Hawatt, M. S. Hamad, K. H. Ahmed, and I. F. El Arabawy. (2013). “Low voltage ride-through capability enhancement of a DFIG wind turbine using a dynamic voltage restorer with Adaptive Fuzzy PI controller”. Proc. 2013 Int. Conf. Renew. Energy Res. Appl. ICRERA 2013, no. October, pp. 1234–1239.
19. “DEVELOPMENT AND APPLICATION OF AN ADVANCED SWITCHED,”. (2006). no. December.
20. G. M. Lee, D. C. Lee, and J. K. Seok. (2004). “Control of Series Active Power Filters Compensating for Source Voltage Unbalance and Current Harmonics”. IEEE Trans. Ind.

Electron., vol. 51, no. 1, pp. 132–139.

21. M. I. Mosaad, M. O. Abed El-Raouf, M. A. Al-Ahmar, and F. M. Bendary. (2019). “Optimal PI controller of DVR to enhance the performance of hybrid power system feeding a remote area in Egypt”. Sustain. Cities Soc., vol. 47, no. February, p. 101469.
22. J. G. Nielsen and F. Blaabjerg. (2005). “A detailed comparison of system topologies for dynamic voltage restorers”. IEEE Trans. Ind. Appl., vol. 41, no. 5, pp. 1272–1280.
23. G. Rashid and M. H. Ali. (2017). “Nonlinear Control-Based Modified BFCL for LVRT Capacity Enhancement of DFIG-Based Wind Farm”. IEEE Trans. Energy Convers., vol. 32, no. 1, pp. 284–295.
24. M. A. A. Yahiya and M. A. R. Uzair. (2016). “Performance analysis of DVR, DSTATCOM and UPQC for improving the power quality with various control strategies,”. Bienn. Int. Conf 2016. Power Energy Syst. Towar. Sustain. Energy.
25. S. Sakar, M. E. Balci, S. H. E. A. Aleem, and A. F. Zobaa.(2016). “Hosting capacity assessment and improvement for photovoltaic-based distributed generation in distorted distribution networks”. EEEIC 2016 - Int. Conf. Environ. Electr. Eng., pp. 2–7.
26. IEEE Std. 519. (2014). “IEEE Recommended Practice and Requirements for Harmonic Control in Electric Power Systems”.